

## REVERSAL OF CARDIAC PATHOLOGY BY ECHOCARDIOGRAPHY IN A DOG WITH SEVERE PULMONARY HYPERTENSION SECONDARY TO HEARTWORM DISEASE - CASE REPORT

Alice RADULESCU<sup>1</sup>, Beatrice CRISTESCU<sup>1</sup>, Pamela HARRIGAN<sup>2</sup>, Lucian IONITA<sup>1</sup>

<sup>1</sup>University of Agronomic Sciences and Veterinary Medicine of Bucharest, Faculty of Veterinary  
Medicine, Bucharest, Romania, alice@medicalvet.ro

<sup>2</sup>Pet Animal Ultrasound Services, Hanson, Massachusetts, USA, 4paus@comcast.net

Corresponding author email: alice@medicalvet.ro

### Abstract

*Canine pulmonary hypertension is a common complication secondary to Heartworm disease. Pulmonary artery occlusion with adult worms, secondary endarteritis, and thromboembolism lead to increased pulmonary pressure and right ventricular pressure with severe consequences on the structure and function of the right heart. Although new advanced diagnostic techniques and new drugs are useful in diagnosis and management, pulmonary hypertension is often an irreversible and progressive disorder. This case report documents the resolution of pulmonary hypertension and subsequent cardiac changes in a dog diagnosed with severe pulmonary hypertension associated with Heartworm disease by 2D, M-mode, and Doppler echocardiography. Comparative echocardiographic assessments performed before and after treatment revealed a rapid reduction in pulmonary pressure and a significant improvement in echocardiographic parameters. Follow-up echocardiographic assessments confirmed the resolution of cardiac changes more than four years after confirmation of the diagnosis.*

**Key words:** Doppler, echocardiography, Heartworm disease, pulmonary hypertension.

### INTRODUCTION

Pulmonary hypertension is a complex syndrome with multifactorial etiology characterized by the increase of pulmonary artery pressure above normal values. In veterinary medicine, pulmonary hypertension is defined as an estimated pulmonary arterial systolic pressure greater than 30 mmHg or pulmonary arterial diastolic pressure greater than 19 mmHg (Johnson et al., 1999; Kellihan and Stepien, 2010). Currently, diseases related to the development of pulmonary hypertension in humans are classified into 5 groups: 1) pulmonary hypertension due to pulmonary arterial vascular disease; 2) pulmonary hypertension due to left heart disease; 3) pulmonary hypertension associated with chronic respiratory disease or hypoxemia; 4) pulmonary hypertension caused by thrombotic or embolic disease and 5) pulmonary hypertension with multifactorial and unclear mechanisms (Galie et al., 2015). These categories have been adapted for use in dogs (Kellihan and Stepien, 2010); however, the number of diseases in each category is much

lower, either because the parallel condition does not occur in dogs or because it is not yet recognized in dogs (Poser and Guglielmini, 2016). Induced by the nematode *Dirofilaria immitis*, Dirofilariosis or Heartworm disease is a common cause of pulmonary hypertension in dogs (Johnson, 1999; Schober and Baade, 2006; Serrano-Parreno et al., 2017). A long-term occlusion of pulmonary arteries leads to pulmonary vascular proliferation, irreversible structural lesions, inflammation, and vascular dysfunction, typical changes for group 1. Conversely, worm death can cause pulmonary embolism and acute signs of pulmonary hypertension, and these are associated with pulmonary hypertension group 4 (Hirano et al., 1992).

The "gold standard" method for measuring pulmonary artery pressure in both humans and animals is right heart catheterization (Kellihan and Stepien, 2010; Galie et al., 2015). In veterinary medicine, catheterization of the heart is an expensive procedure available in a limited number of centers and usually requires deep sedation or anesthesia considered at high risk for unstable patients. Therefore, in veterinary

practice, echocardiography (available and non-invasive) is the standard method used for the diagnosis and monitoring of pulmonary hypertension (Kelliham and Stepien, 2010). Most information is obtained using 2D, M-Mode and Doppler echocardiography. Doppler evaluation of tricuspid regurgitation and pulmonic insufficiency provides an estimation of systolic and diastolic pulmonary arterial pressure, allowing diagnosis and quantification of pulmonary hypertension.

Pulmonary hypertension has been regarded in the past as a rare and incurable condition. In recent years, a better understanding of pathophysiological mechanisms, remarkable technical progress, and new drugs have led to better diagnosis and treatment; however, pulmonary hypertension often remains an irreversible and progressive disorder (Poser and Guglielmini, 2016). In veterinary literature, very few documented echocardiographic cases have been reported about the resolution of cardiac pathology in cases of severe pulmonary hypertension, and these are related to *Angiostrongylus* infection (Esteves et al., 2004), associated with Ehrlichiosis (Den Toom et al., 2016), or with indeterminate causes (Mc Mahon and Saelinger, 2015) but not secondary to Heartworm disease. This case report documents the resolution of pulmonary hypertension and subsequent cardiac changes in a dog diagnosed and treated with severe pulmonary hypertension associated with Heartworm disease by 2D, M-mode, and Doppler echocardiography.

## MATERIALS AND METHODS

Sara, an eight-year-old female spayed Labrador Retriever presented for consultation with a history of intolerance to a minimal effort, dyspnoea, cough and one episode of syncope. Physical examination revealed: weight=32 kg, the rectal body temperature=39.0°C, heart rate=130 bpm and respiratory rate=50 rpm with an abdominal breathing pattern. Pulmonary auscultation showed mild, diffuse crackles. Cardiac auscultation revealed the presence of a grade IV/VI systolic murmur over the tricuspid area. The blood sample was tested serologically with a rapid immunochromatographic test (Snap 4Dx; IDEXX Laboratories), and it was

positive for *D. immitis*. In addition, the microscopic examination found circulating microfilaria which, in the Knott test, were identified as *D. immitis*. Hematology, biochemistry, and urinalysis showed mild eosinophilia, 1.6 K/uL (0.1–1.49 K/uL), mild proteinuria (100 mg/dl) and no other modifications. Electrocardiogram revealed deep S waves in leads II and aVF, right axis deviation and respiratory sinus arrhythmia. Thoracic radiographs showed moderate to severe increase in the size of the pulmonary artery branch, tortuous pulmonary artery branches, enlarged main pulmonary artery, right heart enlargement and moderate to severe patchy perivascular infiltration throughout the lungs. The abdominal ultrasound examination revealed hepatomegaly and liver vein enlargement, no ascites.

After performing the initial tests (physical examination, laboratory investigations, chest radiographs, and abdominal ultrasound), the dog was diagnosed with Heartworm disease class 2. Due to suspected secondary pulmonary hypertension, an echocardiogram was recommended for confirmation, severity, observation of the secondary structural and functional changes, and to assess for the presence of worms in the main pulmonary artery, right ventricle, and/or right atrium. The examination was performed by the same operator with a Logiq P6 ultrasonic machine (General Electric, New York, USA) equipped with a multifrequency array transducer (3 to 5.5 MHz). The dog was not sedated and was positioned in lateral recumbency, being examined in both the right and the left-sided views. Multiple echocardiography methods such as 2D, M-Mode, Color Doppler and Spectral Doppler were used in the evaluation.

### 2D and M-Mode echocardiographic findings

There was a moderate to severe right ventricular dilatation. The average size ratio of right and left ventricular chambers is about 1:3 (Boon 2011). In Sara's case, the right ventricle was markedly dilated, dwarfing the left ventricle. The left ventricular chamber appeared to be smaller than normal, and the free wall and septum were thick, possibly secondary to reduced preload. There was moderate right atrial enlargement and a

curvature of the interatrial septum toward the left atrium consistent with right atrial pressure overload. The right ventricular wall was found to be mildly thickened. Interventricular septal flattening and paradoxical motion consistent with right ventricular pressure overload were present.

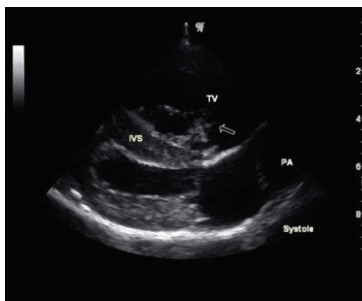
The interventricular septum curved into the left ventricular chamber on long axis view during both phases of the cardiac cycle. (Figure 1A, and 1B), and the flattening of the interventricular septum changed the left ventricular chamber from a circular shape to a triangular or “D”- shaped chamber on short axis view.

Paradoxical septal motion was evaluated using the eccentricity index. Normal eccentricity index during systole and diastole is 1 (one), in that the ventricle maintains its round shape throughout the cardiac cycle (Boon, 2011). In

the subject case the eccentricity index was increased in both systole (1.72) and diastole (1.61) (Figure 2A, and 2B). The main pulmonary artery and left and right branches were dilated. The normal relationship between the pulmonary artery diameter and the aortic root diameter in the dog is less than 0.98 (Serres et al., 2007). In Sara's case, the ratio was 1.33 (Figure 3).

Pulmonic stenosis was ruled out by visualizing pulmonary valve structure and right ventricular outflow tract. Although the parasites can be often visualized echocardiographically in the right heart, pulmonary trunk or right pulmonary branch, in this case, no worms were observed.

The M-Mode measurements (Figure 4) were obtained and compared with M-Mode measurements in healthy Labradors Retrievers (Gugjoo et al., 2014).



A



B

Figure 1. Right parasternal long axis four-chamber view in systole (A) and diastole (B). Severe right ventricular dilation and moderate right atrial enlargement, as well as displacement of the interventricular septum (IVS) and interatrial septum were observed. Right pulmonary artery dilatation (PA) and tricuspid valve (TV) prolapse were noted



A



B

Figure 2. Right parasternal short axis view in systole (A) and diastole (B). The left ventricle (LV) chamber has the shape of "D". The systolic and diastolic eccentricity index, calculated by dividing the width at the left ventricular chamber height, were increased (EI sys. = 1.72, EI dias. = 1.61)



Figure 3. Right parasternal short axis view. The main pulmonary artery (PV) is dilated and the ratio between main pulmonary artery diameter and aortic root (Aov) was increased (MPA:Ao = 1.33)

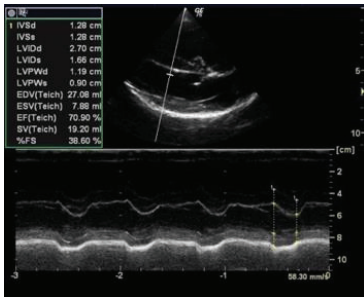


Figure 4. Right parasternal long axis four-chamber view M-Mode measurements. There was a reduced left ventricular diastolic diameter (LVDd = 27.0 mm, normal 37.58±1.05 mm), a reduced left ventricular systolic diameter (LVDs = 1.66 mm, normal 23.9±0.97 mm), a thickened interventricular septum in diastole (IVSd = 12.8 mm, normal 9.06±0.37 mm) and a thickened left ventricular free wall in diastole (LVPWd = 11.9 mm, normal 8.75±0.26 mm).

### Doppler assessment of systolic pulmonary arterial pressure

Tricuspid regurgitation was present, secondary to the annular stretch and changes in right ventricular geometry. Tricuspid valve regurgitation occurred during ventricular systole and was viewed in the right parasternal and left apical views. The tricuspid regurgitation jet was assessed by using Color Doppler (Figure 5). CW Doppler was placed over the tricuspid regurgitation jet to obtain tricuspid velocity profiles. To achieve an accurate reading of the velocity, care was taken to have proper alignment of the CW Doppler cursor on the regurgitant jet direction. In our case, the best alignment was found in the right parasternal view and maximum velocity of the tricuspid regurgitant jet measured as  $v=4.52$  m/s (Figure 6). By using the maximum

tricuspid regurgitation velocity, the pressure across the tricuspid valve was calculated, which approximated the pressure between the right ventricle and right atrium. This pressure gradient is calculated by applying the measured maximum tricuspid regurgitation velocity to the modified Bernoulli equation as follows:  $pressure\ gradient = 4 \times 4.52^2 = 81.84\ mmHg$ . The right ventricular pressure was estimated by adding to the calculated pressure gradient the estimated right atrial pressure. Right atrial pressure was estimated based on subjective assessment of the right atrium size. Because in our case the right atrium was moderately increased, an estimated right atrial pressure of 10 mmHg was used. The right ventricular systolic pressure which is normally equal with pulmonary systolic pressure calculated to be 91.84 mmHg, markedly elevated (normal pulmonary artery systolic pressure is approximately 20-25 mmHg).

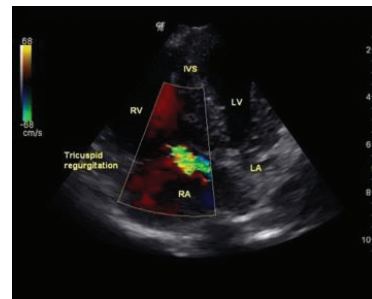


Figure 5. Left apical four-chamber view Color Doppler. The presence of eccentric tricuspid regurgitation jet was visualized

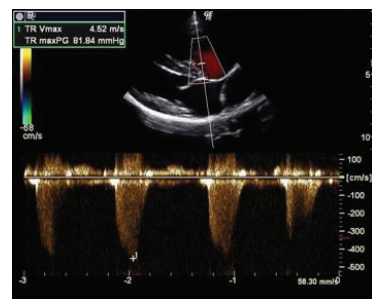


Figure 6. Right parasternal long axis four chamber view CW Doppler. The maximum tricuspid regurgitation velocity measured 4.52 m/s

### Doppler assessment of diastolic pulmonary arterial pressure

Pulmonary valve insufficiency occurred in diastole and was best observed in the right parasternal short axis view. In this view, the pulmonary insufficiency jet assessed by Color Doppler. CW Doppler was placed over the pulmonary insufficiency jet to obtain pulmonary insufficiency velocity profiles. The pulmonary insufficiency velocity was measured to be  $v=3.08$  m/s (Figure 7). Applying the modified Bernoulli equation, the pressure difference between the pulmonary artery and right ventricle was calculated:  $pressure\ gradient = 4 \times 3.08^2 = 38.05\ mmHg$ . The right ventricular pressure in diastole was assumed to be 0 mmHg; thus, the pressure gradient across the pulmonary valve in diastole was considered equal with diastolic pulmonary artery pressure. In this case, the calculated diastolic pulmonary artery pressure was 38.05 mmHg, which is high compared to the normal pulmonary artery pressure at the end of diastole of about 6-10 mmHg.

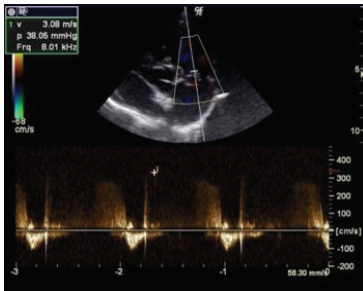


Figure 7. Right parasternal short axis view at the level of aorta and pulmonary artery. The pulmonic insufficiency velocity measured with CW Doppler was increased at 3.08 m/s

### Doppler assessment of pulmonary flow profile

The pulmonary flow velocity profile was subjectively assessed and classified as type III (asymmetric profile and notching appears in the ascending section of the envelope) suggestive for severe PH (Boon, 2011).

### Diagnosis and Treatment

Based on Sara's echocardiographic examination, the diagnosis of severe pulmonary hypertension secondary to *D. immitis* infection was confirmed. The initial established

therapeutic protocol was as follows: Prednisolone 1 mg/kg/day (the dose gradually reduced, and administration interval increased) for the reduction of inflammatory reactions and the treatment of allergic pneumonia; Doxycycline 10 mg/kg/day four weeks to eliminate the endosymbiont *Wolbachia*; Sildenafil 1.5 mg/kg twice daily for reducing vascular resistance and pulmonary pressure; Ivermectin 6 mcg/kg every three weeks to kill immature larvae and microfilaria; Benazepril 0.25 mg/kg twice daily and Furosemide 1 mg/kg twice daily for right heart failure symptoms. Oxygen supplementation and cage rest recommended. After one and a half months of treatment, Sara presented for reassessment. She was reported to be very well at home with regular activity, normal appetite, and normal breathing.

Physical examination revealed the resolution of right-sided murmur, a normal respiratory pattern and normal bronchovesicular sounds. Echocardiography showed a significant reduction in pulmonary hypertension and a marked improvement in cardiac changes that had been observed initially. 2D and M-Mode examination showed mild right ventricular and right atrial dilation, normal left ventricular dimension with normal left ventricular and interventricular septum wall thickness (Figure 8), resolution of normal septal configuration without septal flattening, normal eccentricity index (EI) both in systole and diastole (Figure 9), normal main pulmonary artery to aorta ratio (MPA: Ao).

The M-Mode measurements obtained were compared to normal M-Mode values in healthy Labradors (Gugjoo et al., 2014), and found to be normal (Figure 10). The Color Doppler examination revealed the presence of a trivial tricuspid regurgitation jet (Figure 11), as well as a trace pulmonary insufficiency jet (Figure 12) with a low-velocity flow that could not be accurately measured. In the absence of tricuspid regurgitation and pulmonary insufficiency, in order to detection and grading of pulmonary hypertension were used systolic time intervals (AT, ET, AT:ET) (Figure 13) (Schober and Baade, 2006), right pulmonary artery distensibility index (RPAD Index) (Figure 14) (Venco et al., 2014), and tricuspid annular plane systolic excursion (TAPSE)

(Figure 15) (Pariat et al., 2012); all these indicators were found to be normal.

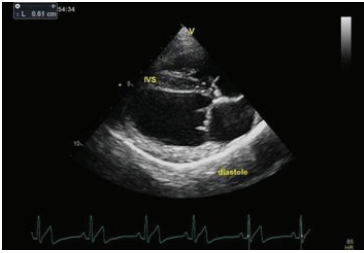


Figure 8. Right parasternal long axis-four chamber view. Mild right ventricular dilatation; no septal flattening



Figure 9. Right parasternal short axis view at the level of papillary muscles in diastole. The left ventricle has a normal circular shape; eccentricity index normal EI diastolic = 1.07

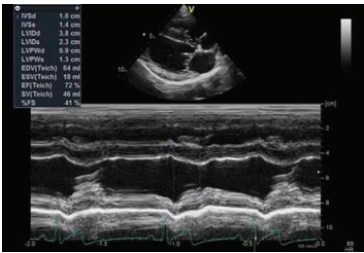


Figure 10. Right parasternal long axis four-chamber view M-Mode. There was a normal left diastolic diameter (LVDd = 3.8 cm) and a normal wall thickness (LVWd = 0.9 cm). No septal flattening observed

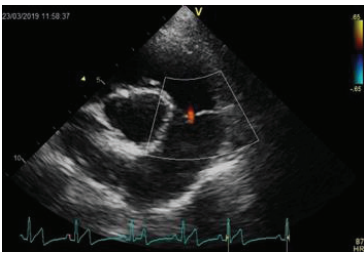


Figure 11. Right parasternal short axis view at the level of aorta and pulmonary artery. By using Color Doppler, the presence of trace pulmonic insufficiency with low velocities visualized

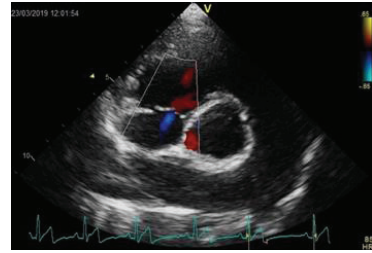


Figure 12. Right parasternal short axis view at the level of tricuspid valve. By using Color Doppler, the presence of trivial tricuspid regurgitation with low velocities visualized

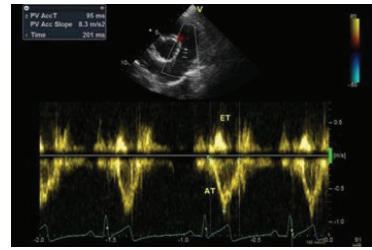


Figure 13. Right parasternal short axis view at the level of pulmonary artery PW Doppler. The pulmonary outflow acceleration time (AT), ejection time (ET) measured, and the ratio AT:ET calculated. The values are normal; ET =201 ms, AT =95 ms, AT:ET = 0.47

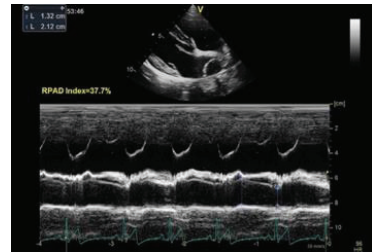


Figure 14. Right parasternal long axis view adapted for right pulmonary artery M-Mode. The Right Pulmonary Artery Distensibility Index (RPAD Index) calculated and normal value was found RPAD Index = 37.7%

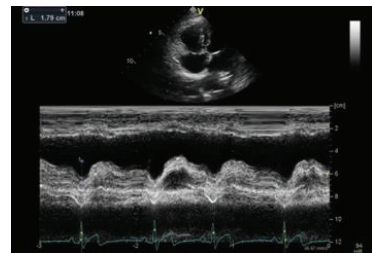


Figure 15. Left apical four chamber adapted for lateral tricuspid annulus M-Mode. Tricuspid annular plane systolic excursion (TAPSE) was acquired. Normal value was found TAPSE = 1.79 cm

With the resolution of right heart failure symptoms and significant reduction in pulmonary artery pressure, the treatment for right heart failure was discontinued and the dose of Sildenafil was reduced at 1mg/kg twice daily. According to AHS (American Heartworm Society) and ESDA (European Society of Dirofilariosis and Angiostrongylosis) recommendation, after patient preparation with Ivermectin and Doxycycline, adulticide protocol was initiated. The Melarsomine was administered as a deep intramuscular injection in dorsal lumbar musculature. One injection (2.5 mg/kg) was administered to kill the most sensitive adult worms. After one month from the first injection with Melarsomine, two more injections were administered 24 hours apart. For the entire period, Sara was in strict cage rest. About six months after Melarsomine treatment, the dog showed a negative result to the Heartworm antigen test. Following the adulticide protocol, the pulmonary damage did not aggravate, and the signs of pulmonary hypertension did not recur. The subsequent echocardiographic assessments over a four-year period confirmed the resolution of pulmonary hypertension and secondary cardiac changes.

## RESULTS AND DISCUSSION

By correctly interpreting Doppler measurements and integrating 2D and M-mode echocardiographic results, pulmonary hypertension can be more accurately evaluated, leading to a better understanding of the pathophysiology of the disease. In our case, based on tricuspid regurgitation and pulmonary insufficiency, pulmonary arterial systolic pressure was estimated to be approximately 91.84 mmHg and pulmonary arterial diastolic pressure of about 38.05 mmHg, these values being very high compared to normal. The presence and severity of pulmonary hypertension were also assessed indirectly by identifying two-dimensional (2D) and time-motion (M-Mode) echocardiographic abnormalities, confirming pulmonary hypertension with significant cardiac pathology. Observed were: severe right ventricular dilatation with mild right ventricular wall thickness, moderate right atrial dilatation, severe interventricular septal flattening and paradoxical motion, moderate to

severe pulmonary arterial dilatation and decrease left ventricular volume with subjective thickening of the walls.

The structural characteristics of the right ventricle allow for good adaptation to large increases in blood volume (preload), but not to a rapid increase in arterial resistance (afterload).

Typically, the increase in pulmonary arterial resistance results in increased right ventricular contractility and subsequent concentric hypertrophy. If the size or rate of increase in pulmonary arterial pressure is too high, this mechanism fails and leads to an increase in the internal diameter of the right ventricle (eccentric hypertrophy) (Gaynor et al., 2005). The degree of concentric hypertrophy compared to eccentric hypertrophy can give information about chronicity and the possible causes of pulmonary hypertension. Severe concentric right ventricular hypertrophy is particularly common in chronic conditions, whereas severe eccentric right ventricular hypertrophy, is usually seen in acute conditions (Roberts and Forfia, 2011). In the subject case, there were no findings of compensatory hypertrophy, and in consequence, the assumption was that Sara had a poor compensatory response due to the acute increase in pulmonary pressure.

Comparative clinical and echocardiographic evaluations before and after treatment showed rapid resolution of the clinical signs and a marked improvement in the echocardiographic parameters. There were found: normal right ventricular and right atrial chamber, normal septal configuration both in diastole and systole, normal flow profile in the right ventricular ejection tract, and trace tricuspid regurgitation and pulmonic insufficiency with low velocities flow that could not be accurately measured.

In the absence of tricuspid regurgitation and pulmonic insufficiency, indicators such as Tricuspid Annular Plane Systolic Excursion (TAPSE), Acceleration Time (AT) and its ratio to pulmonary artery Ejection Time (AT:ET), and Right Pulmonary Artery Distensibility Index (RPAD Index), were used to assess pulmonary hypertension and were found to be normal. In dogs, one study showed that TAPSE was correlated with the severity of pulmonary

hypertension with different causes (Pariat et al., 2012). In another study, AT and AT: ET were useful indicators for predicting pulmonary hypertension in West Highland White Terriers with chronic pulmonary disease (Schober and Baade, 2006). The RPAD Index was predictive of pulmonary hypertension and very correlated with invasively measured pulmonary arterial pressure in dogs with Heartworm disease

(Venco et al., 2014). In our case, the RPAD Index was found at the normal upper limit, and the Windkessel effect characteristic of normal pulmonary artery morphology was not clearly, suggesting, however, the loss of elasticity of the arterial wall. Subsequent evaluations for about four years did not reveal recurrence, and the dog continued to be clinically healthy and normal echocardiographically. (Table 1).

Table 1. Echocardiographic measurement

| Echocardiographic examination | First examination | 1.5 months after | 6 months after   | 1.5 year after   | 4 years after    | Normal echocardiographic parameters      |
|-------------------------------|-------------------|------------------|------------------|------------------|------------------|--|
| <b>M-Mode parameters</b>      |                   |                  |                  |                  |                  |  |
| RVWd (mm)                     | 6.7               | 6.5              | 6.2              | 6.1              | 6.1              |  |
| IVSd (mm)                     | 12.8              | 10.0             | 10.0             | 11.0             | 10.0             | 9.06±0.37<br>(Gugjoo et al., 2014)       |
| LVWd (mm)                     | 11.9              | 10.0             | 10.0             | 10.0             | 9.0              | 8.75±0.26<br>(Gugjoo et al., 2014)       |
| LVDd (mm)                     | 27.0              | 38.0             | 38.0             | 36.0             | 38.0             | 37.58±1.05<br>(Gugjoo et al., 2014)      |
| LVDs (mm)                     | 16.6              | 22.0             | 22.0             | 20.0             | 23.0             | 23.98±0.97<br>(Gugjoo et al., 2014)      |
| FS %                          | 38.6              | 42               | 42               | 45               | 41               | 35.89±1.56<br>(Gugjoo et al., 2014)      |
| <b>B Mode Parameters</b>      |                   |                  |                  |                  |                  |  |
| EI dias.                      | 1.61              | 1.1              | 1,14             | 1,07             | 1,07             | Aprox 1.0 (Ryan et al., 1985)            |
| EI sys.                       | 1.72              | 1.2              | 1.14             | 1.10             | 1.18             | Aprox 1.0 (Ryan et al., 1985)            |
| MPA (mm)                      | 29.3              | 27.5             | 24.1             | 23.7             | 23.3             |  |
| Ao (mm)                       | 22.0              | 23.3             | 24.2             | 23.9             | 24.2             | 23.71±0.48<br>(Gugjoo et al., 2014)      |
| MPA/Ao                        | 1.33              | 1.18             | 0.99             | 0.99             | 0.96             | <0.98 (Serres et al., 2007)              |
| <b>CW Doppler</b>             |                   |                  |                  |                  |                  |  |
| vTR (m/s)<br>PASP (mmHg)      | 4.52<br>91.84     | 2.8<br>36.36     | Trivial jet<br>- | Trivial jet<br>- | Trivial jet<br>- | <2.8 (Kellihan and Stepien, 2010)<br><30 |
| vPI (m/s)<br>PADP (mmHg)      | 3.08<br>38.05     | 1.83<br>13.39    | 1.81<br>13.10    | 1.59<br>10.11    | Trivial jet<br>- | <2.2 (Kellum and Stepien, 2007)<br><19   |
| <b>PW Doppler</b>             |                   |                  |                  |                  |                  |  |
| vPAmox (m/s)                  | 1.19              | 1.04             | 0.94             | 0.86             | 0.91             | <1.3 (Boon, 2011)                        |

RVWd: right ventricular wall in diastole; IVSd: interventricular septum in diastole; LVWd: left ventricular wall in diastole; LVDd: left ventricular diameter in diastole; LVDs: left ventricular diameter in systole; FS: fractional shortening; EI dias.: diastolic eccentricity index; EI sys.: systolic eccentricity index; MPA: main pulmonary artery; Ao: aorta; MPA/Ao: main pulmonary artery to aorta ratio; vTR: tricuspid regurgitation velocity; PASP: pulmonary artery systolic pressure; vPI: pulmonic insufficiency velocity; PADP: pulmonary artery diastolic pressure; vPAmox: maximum velocity through the pulmonary artery.

The aim of the treatment was first to stabilize the patients and then treat the causes. The acute onset of clinical signs has been attributed to the recent natural death of one or more parasites, dead worms, along with inflammation and platelet aggregation, leading to pulmonary thromboembolism, a sudden increase in pulmonary pressure, and development of acute signs of right heart failure. Although the initial therapeutic protocol was complex and each drug had its role; it was assumed that treatment with Prednisolone resulted in a significant reduction in the inflammatory response and contributed to the control of clinical signs of thromboembolism (Atwell and Tarish, 1995). Doxycycline, used to eliminate *Wolbachia*, was also an essential part of the treatment, this endo-symbiotic bacteria being an important factor in the occurrence of severe inflammatory response (Frank and Heald, 2010). Recent studies have shown a decrease in gross and microscopic pathology of pulmonary parenchyma in experimental Heartworm disease pretreated with Doxycycline before Melarsomine administration (Nelson et al., 2017). It was also appreciated that in this case, Sildenafil played an important therapeutic role, contributing to the reduction of pulmonary pressure and was associated with improvement in clinical signs. Studies conducted in canine models with pulmonary thromboembolism have shown that Sildenafil produces selective pulmonary vasodilation resulting in attenuation of pulmonary hypertension (Souza-Silva et al., 2005; Dias-Junior and Tanus-Santos, 2006). In some studies on the efficacy of Sildenafil in the treatment of pulmonary hypertension in dogs, pulmonary pressure reduction has been demonstrated (Bach et al., 2007; Brown et al., 2010), solving syncopal events, increasing exercise tolerance and improving quality of life (Kellum and Stepien, 2007; Toyoshima et al., 2007). Although, in Heartworm disease, therapeutic management involves certain risks, in our case, after adulticide treatment, no recurrence of pulmonary hypertension has been revealed. Otherwise, in a recent study of Heartworm disease in dogs, echocardiographic parameters were followed before and after adulticide treatment recommended by the American Heartworm Society, and no

worsening was observed (Serrano-Parreno et al., 2017).

In this case, the reasons for the significant improvement in clinical signs and resolution of the structural and functional changes of the heart, remain speculative. We can assume that a number of factors have contributed, including the degree of cardiopulmonary compromise (although severe, cardiac changes were acute, and therefore, perhaps, reversible) and patient response to therapy, both for cause and effect. Due to the potential for rapid and irreversible damage to pulmonary vasculature and right heart, pulmonary hypertension is a disease that needs to be investigated, recognized and treated appropriately. Although remarkable progress has been made in the diagnosis and therapy of the disease, more time and further studies are necessary for a better approach to this condition.

## REFERENCES

- Atwell R., Tarish JH., 1995. *The effect of oral low-dose prednisolone on the extent of pulmonary pathology associated with dead Dirofilaria immitis in a canine lung model*. Proceedings of the heartworm symposium '95, pp.103–111 ref.28, American Heartworm Society, Batavia.
- Bach JF., Rozanski EA., MacGregor J., Betkowski JM., Rush JE., 2006. *Retrospective evaluation of sildenafil citrate as a therapy for pulmonary hypertension in dogs*. J Vet Intern Med. 20(5): 1132-5.
- Boon J.A., 2011. *Veterinary echocardiography second edition*. Ed. Wiley-Blackwell, Ames, Iowa.
- Brown AJ., Davison E., Sleeper MM., 2010. *Clinical efficacy of sildenafil in treatment of pulmonary arterial hypertension in dogs*. J Vet Intern Med. 24(4): 850-4.
- Den Toom ML., Dobak TP., Broens EM., Valtolina C., 2016. *Interstitial pneumonia and pulmonary hypertension associated with suspected ehrlichiosis in a dog*. Acta Vet Scand 58:46.
- Dias-Junior CA., Tanus-Santos JE., 2006. *Hemodynamic effects of sildenafil interaction with a nitric oxide donor compound in a dog model of acute pulmonary embolism*. Life Sci. 2006 Jun 27;79(5):469-74.
- Estèves I., Tessier D., Dandrieux J., Polack B., Carlos C., Boulanger V., Muller C., Pouchelon JL., Chetboul V., 2004. *Reversible pulmonary hypertension presenting simultaneously with an atrial septal defect and angiostrongylosis in a dog*. J Small Anim Pract. 45:206–9.
- Frank K., Heald R.D., 2010. *The emerging role of Wolbachia species in heartworm disease*. Compend Contin Educ Vet. 32(4):E4.
- Galie N., Humbert M., Vachiery JL., Gibbs S., Lang I., Torbicki A., Simonneau G., Peacock A., Noordegraaf

- AV., Begheti M., Gaynor SL., Maniar HS., Bloch JB., Steendijk P., Moon MR., 2005. *Right atrial and ventricular adaptation to chronic right ventricular pressure overload*. *Circulation* 112 (9 Suppl): 1212-8.
- Ghofrani A., Sanchez MAG., Hansmann G., Klepetko W., Lancellotti P., Matucci M., McDonagh T., Pierard LA., Trindade PT., Zompatori M., Hoepfer M., ESC Scientific Document Group., 2015. *Guidelines for the diagnosis and treatment of pulmonary hypertension*. *European Heart Journal*. 37(1): 67-119.
- Gugjoo MB., Hoque M., Saxena AC., Schamsuz MM., Dey S., 2014. *Reference values of M-mode echocardiographic parameters and indices in conscious Labrador Retriever dogs*. *Iranian Journal of Veterinary* 15(4): 341-346.
- Hirano Y., Kitagawa H., Sasaki Y., 1992. *Relationship between pulmonary arterial pressure and pulmonary thromboembolism associated with dead worms in canine heartworm disease*. *J Vet Med Sci* 54(5): 897-904.
- Johnson L., 1999. *Diagnosis of pulmonary hypertension*. *Clin Tech Small Anim Pract*. 14(4): 231-6.
- Johnson L., Boon J., Orton EC., 1999. *Clinical characteristics of 53 dogs with Doppler-derived evidence of pulmonary hypertension: 1992-1996* *J Vet Intern Med* 13(5): 440-7.
- Kelliham HB., Stepien RL., 2010. *Pulmonary hypertension in dogs: diagnosis and therapy*. *Vet Clin North Am Small Anim Pract*. 40(4): 623-41.
- Kellum HB., Stepien RL., 2007. *Sildenafil citrate therapy in 22 dogs with pulmonary hypertension*. *2007 J Vet Med* 21(6) 1258-64.
- Mc Mahon P., Saelinger C., 2015. *Reversal of echocardiographic right-sided heart pathology in a dog with severe pulmonary hypertension: a case report*. *Vet Med: Research and Reports* 6: 211-218.
- Nelson CT., Myrick ES., Nelson TA., 2017. *Clinical benefits of incorporating doxycycline into a canine heartworm treatment protocol*. *Parasites & Vectors* 10 (2):515.
- Pariaut R., Saelinger C., Strickland KN., Beaufre H., Reynolds CA., Vila J., 2012. *Tricuspid annular plane systolic excursion (TAPSE) in dogs: reference values and impact of pulmonary hypertension*. *J Vet Intern Med* 26(5): 1148-54.
- Poser H., Guglielmini C., 2016. *Pulmonary Hypertension in the dog* *Acta Veterinaria-Beograd* 66(1): 1-25.
- Roberts DJ., Forfia PR., 2011. *Diagnosis and assessment of pulmonary vascular disease by Doppler echocardiography*. *Pulmonary Circulation* 1(2) 160-181.
- Schober KE., Baade H., 2006. *Doppler echocardiographic prediction of pulmonary hypertension in West Highland white terriers with chronic pulmonary disease*. *J Vet Intern Med* 20(4): 912-20.
- Serrano-Parreno B., Carreton E., Caro-Vadillo A., Falcon-Cordon S., Falcon-Cordon Y., Montoya-Alonso JA., 2017. *Pulmonary hypertension in dogs with heartworm before and after the adulticide protocol recommended by the American Heartworm Society*. *Vet Parasitol*. 236:34-37.
- Serres F., Chetboul V., Gouni V., Tissier R., Sampedrano CC., Pouchelon JL., 2007. *Diagnostic value of echo-Doppler and tissue Doppler imaging in dogs with pulmonary arterial hypertension*. *J Vet Intern Med*. 21(6):1280-9.
- Souza-Silva AR., Dias-Junior CA., Uzuelli JA., Moreno H Jr., Evora PR., Tanus-Santos JE., 2005. *Hemodynamic effects of combined sildenafil and L-arginine during acute pulmonary embolism-induced pulmonary hypertension*. *Eur J Pharmacol*. Nov 7;524(1-3):126-31.
- Toyoshima Y., Kanemoto I., Arai S., Toyoshima H., 2007. *A Case of Long-Term Sildenafil Therapy in a Young Dog with Pulmonary Hypertension*. *Journal of Veterinary Medical Science* 69(10): 1073-5.
- Venco L., Mihaylova L., Boon JA., 2014. *Right Pulmonary Artery Distensibility Index (RPAD Index). A field study of an echocardiographic method to detect early development of pulmonary hypertension and its severity even in the absence of regurgitant jets for Doppler evaluation in heartworm-infected dogs*. *Vet Parasitology* 15;206 (1-2): 60-6.